Conference paper

Raul Losantos, Diego Sampedro and María Sandra Churio*

Photochemistry and photophysics of mycosporine-like amino acids and gadusols, nature's ultraviolet screens

DOI 10.1515/pac-2015-0304

Abstract: Mycosporine-like amino acids (MAAs) and related gadusols are among the most prominent examples of metabolites suggested to act as UV-sunscreens. This review illustrates how experimental and theoretical studies on model MAAs and gadusol offer a helpful description of the photoprotective mechanism at the molecular level. This knowledge may contribute to the rational design of chemical systems with predictable and tuneable response to light stimulus. Synthetic efforts to obtain MAAs and simplified related structures are also discussed.

Keywords: computational chemistry; laser spectroscopy; natural products; organic chemistry; Photobiology-16; photoprotection; sunscreens; synthesis.

Introduction

Since the late 1970s, hundreds of publications have addressed the isolation, structural elucidation, occurrence and roles of mycosporine and mycosporine-like amino acids (MAAs). These are two groups of secondary metabolites synthesized by cyanobacteria, fungi, algae and ingested or accumulated by high order animals such as fish, cnidarians, arthropods, molluscs, and echinoderms [1, 2]. Several hypotheses about the role of these compounds in biological systems have been formulated and are still on discussion. Among other functions, osmotic and reproduction regulation, UV transduction in photosynthesis, intracellular nitrogen reservoir and ecological connectivity have been suggested [3–5]. The MAAs in particular have been recognized as molecules of key significance in marine ecosystems [6]. Beyond the controversy about their multifunctionality, MAAs have mainly attracted interest around their role as UV sunscreens in a wide variety of organisms [4, 7–9].

Mycosporine and MAAs are water soluble compounds; their basic chemical structure contains a cyclohexenone or a cyclohexenimine unit (Fig. 1). Fungal mycosporines and only two MAAs from marine sources (mycosporine-glycine and mycosporine-taurine) consist of a cyclohexenone ring system linked to an amino acid, with maximal absorption between 310 and 320 nm. The rest of the MAAs generally includes a glycine moiety attached to a cyclohexenimine ring and a second substituent group (amino acid, amino alcohol or an

Article note: A collection of invited papers based on presentations at the 16th International Congress on Photobiology (ICP-16), Córdoba, Argentina, 7–12 September 2014.

***Corresponding author: María Sandra Churio,** Facultad de Ciencias Exactas y Naturales, Departamento de Química, Universidad Nacional de Mar del Plata, Consejo Nacional de Investigaciones Científicas y Técnicas (CONICET), Dean Funes 3350, B7602AYL, Mar del Plata, Argentina, e-mail: schurio@mdp.edu.ar; sanchurio@hotmail.com
Raul Losantos and Diego Sampedro: Departamento de Química, Universidad de La Rioja, Centro de Investigación en Síntesis Química (CISQ), Madre de Dios, 51, 26006 Logroño, Spain

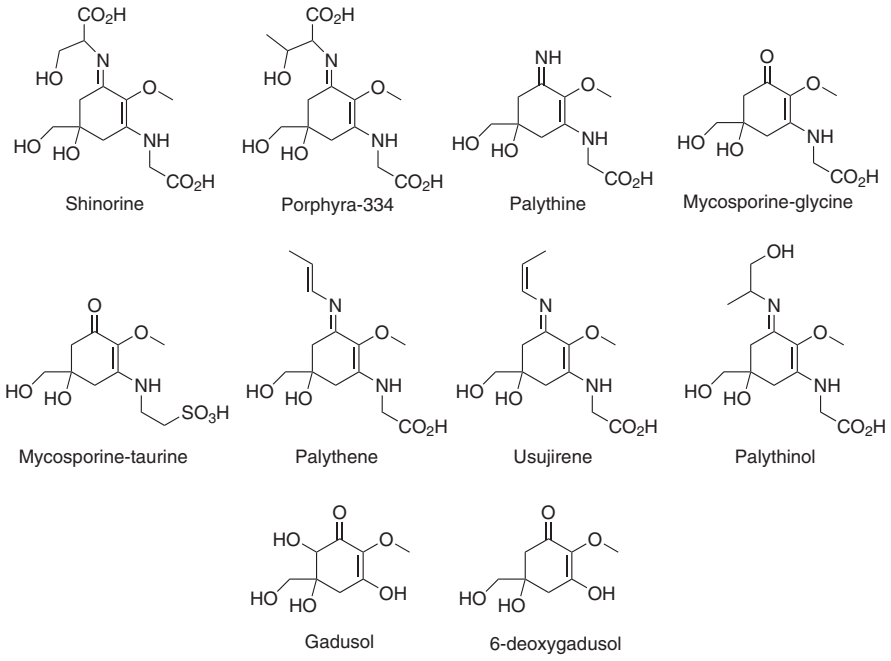

Fig. 1: Chemical structures of some relevant MAAs and gadusols.

enaminone system). This results in a diversity of more than 20 structures with UV-absorption bands at maximum wavelengths from 320 nm to *ca*. 360 nm and molar absorptions coefficients in the range from 28 000 to 60 000 M^{-1} cm^{-1} [7]. In fact, MAAs have been considered as the strongest UVA absorbing compounds in nature.

On the other hand, related compounds such as gadusol and deoxygadusol (Fig. 1) are natural cyclohexenones resembling the mycosporine core. They absorb intensively towards the UVB and UVC spectrum with pH-dependent distinctive maxima: 269 (pH 2) and 296 (pH 7) [10, 11].

Both compounds are generally involved as intermediates in the proposed schemes for MAAs biosynthesis [2, 8, 12]. Their role in UV photoprotection is particularly relevant from an evolutionary point of view since primitive organisms that developed in the absence of atmospheric O_2 may have required UVB/C screening, hypothetically fulfilled by gadusols and oxo-mycosporines [13].

UV-induced synthesis and accumulation have been broadly reported and generally regarded as central evidence supporting the sunscreening role of MAAs in living organisms [4, 14–17]. However the chemistry and molecular basis of the photoprotective potential of MAAs and gadusols have been examined to a lesser extent.

The exploration of the basic photochemical and photophysical features of MAAs is important for the understanding of natural mechanisms of photoprotection which becomes particularly significant in the context of the stratospheric ozone depletion phenomenon and the consequent effects of UV radiation on living beings [18]. This problematic has led to consider MAAs and other natural photoprotective molecules as valued alternatives to synthetic compounds for the formulation of topical sunscreens [19, 20]. Besides, the characterization at a molecular level of the light induced behaviour of this family of compounds may help to designing derivatives for future applications in the cosmeceutical and pharmaceutical industries [21, 22].

In this work we review the in vitro experimental studies and theoretical calculations reported to date on the photochemistry and photophysics of MAAs and gadusols.

Mycosporine-like amino acids

As seen, MAAs are low-molecular-weight, generally colorless and water-soluble compounds that are also resistant to thermodegradation and photodegradation under environmental conditions. Most of the photo-

physical and photochemical properties of these molecules are quite general and independent of the specific substituents linked to the core structure. Thus, general aspects will be described in the following sections with specific examples to illustrate the behavior of these compounds.

Photophysical properties

UV-Vis absorption

One of the most relevant features of the MAAs is their high UV-absorbing capability, due to a single band centered in the 310–360 nm range, partially covering the harmful UVA and UVB radiations zones. This strong absorption reaches molar absorption coefficients between 20 000 and 40 000 L cm^{-1} mol^{-1} which may rise over 50 000 in cases such as that of palythene [7]. Depending on the origin, relevant differences between the compounds found in algae and those found in fungi have been reported. In fungi metabolites, the chromophore is less conjugated and in all cases it shows a maximum near 310 nm, practically without dependence on the amino-substitution [9].

In all marine MAAs a similar behavior is observed with an absorption maximum *ca*. 320 nm for the non-substituted imino-MAAs and *ca*. 360 nm for the substituted ones. In this case, the substituents may be important as they can modify the chromophore's conjugation. In turn, this allows for the modulation of their UV-Vis spectral properties, yielding a bathochromic shift when conjugation increases. When conjugated C=C bonds are directly linked to the chromophore, the *Z*-isomer shows an hypsochromic shift relative to the *E*-isomer of 2–3 nm, as in usujirene and palythene (Fig. 1) [23]. A non-common behavior is found for the *E*–*Z*-palythenic acid pair, in which the *E*-isomer is 2 nm blue-shifted [24].

Due to the amino acidic structure, a zwitterionic character is expected. It is unclear if the relevant form in vivo is the anionic, the "neutral" or zwitterionic or the protonated one. To try to clarify this aspect porphyra-334 was studied at different pH values [25]. It was found that in high acidic aqueous solution (pH 1–3) the absorption maximum of porphyra-334 shows a hypsochromic shift from 332 nm at pH 3 and to 330 nm at pH 1 and pH 2. Under these conditions, the molar absorption coefficient also decreases with higher acidity. As other MAAs, porphyra-334 is a zwitterion that presents two acidic groups and one iminic nitrogen as shown in Fig. 2. When the pH is below 3, the π delocalization is not possible due to the protonation of the non-bonding pair in the nitrogen atom. Subsequent protonation of the acidic groups may take place at lower pH values.

On the other hand, the absorption maximum and molar absorption coefficient of porphyra-334 do not change in alkaline solutions. This is reasonable since both acidic groups do not alter the electronic properties of the chromophore as they are not directly bonded to it.

The behavior of porphyra-334 under acidic conditions was further explored by computing the gas phase proton affinity [26]. For this compound, a value of 266 kcal mol^{-1} was found which is in the range of the gas phase proton affinity of certain artificial super-bases. This turns porphyra-334 into a so-called "*proton sponge*." The term refers to species with exceptionally high proton affinities which seem to be related to the high stability of this compound in very acidic water solutions. In contrast, under relatively low basic conditions of pH

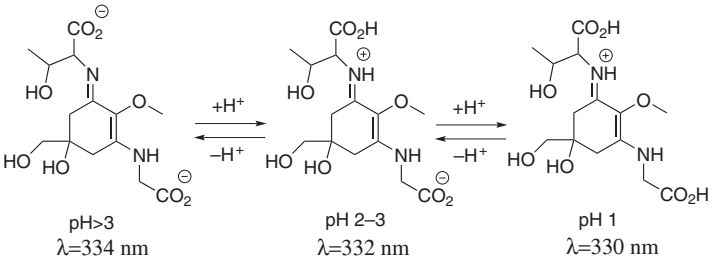

Fig. 2: Molecular structures of porphyra-334 at different pH values.

12, porphyra-334 decomposes rapidly to give unknown products [25]. The reasons behind this feature were explained in terms of positive charge delocalization between the two nitrogen atoms and the alkene moiety that connects them. This type of push–pull charge stabilization has been previously proposed for other types of compounds showing also high proton affinity. Significantly, this proton-capturing ability is comparable to that one of other artificial systems specifically designed to behave like this [27]. Other MAAs show also small solvent dependence in the UV absorption with changes within 2–4 nm in many of them [28, 29].

Fluorescence emission

In contrast to the UV absorption properties, results from fluorescence measurements on MAAs are only available for the most studied compounds, namely porphyra-334, shinorine and palythine. These three molecules were characterized by steady-state spectrofluorometry in aqueous solutions with monochromatic irradiation at the absorption maximum and by time-correlated single photon counting (TCSPC) for the determination of the singlet state lifetimes.

One of the better known MAAs, porphyra-334, was first isolated from the red alga *Porphyra tenera* [30]. However, it took more than 20 years to thoroughly explore its excited-state properties [28]. The results from TCSPC for porphyra-334 in aqueous solution evidence an excited-state with a short lifetime of 0.4 ns. Besides, no longer lived transient species were detected after irradiation at the absorption maximum. The emission spectrum consists of a weak band centered at 395 nm which amounted a very low fluorescence quantum yield ($\Phi_F = 2.0 \times 10^{-4}$) [28, 31].

Structurally very similar to porphyra-334, shinorine is usually found in the same organisms but sometimes in larger amounts (Fig. 1). It has been obtained from adult sea urchins eggs as methanolic extracts [32]. Detailed photophysical studies on shinorine indicated that, as porphyra-334, this metabolite efficiently dissipates light energy into heat [31]. Shinorine also shows a very low fluorescence quantum yield ($\Phi_F = 1.6 \times 10^{-4}$) and a short fluorescence lifetime (0.35 ns). The emission spectrum exhibits a very weak maximum around 386 nm.

Palythine is the MAA with the simplest structure. It was first isolated from the zoanthid *Palythoa tuberculosa* [33]. The structures of palythine and other related compounds (mycosporine-glycine, palythinol and palythine) obtained from the same source were later proposed (Fig. 1) [34]. A very detailed photophysical analysis of palythine in water has been performed [35]. The lack of measurable luminescence implies a very efficient deactivation pathway. The weak emission band experimentally observed was attributed to an impurity and not to palythine.

According to these results, the suggested role of MAAs as transducers of the UV light to more useful wavelengths in the photosynthesis seems quite improbable due to the very low observed fluorescence quantum yields.

Triplet excited state

As with fluorescence, the absorption features, formation yield and the energy of the triplet state have been only determined for a few MAAs.

Laser-flash photolysis experiments have allowed for the characterization of the excited triplet state of shinorine [31], porphyra-334 [28] and palythine [35]. Data for the triplet-triplet energy transfer from 1-naphthalene-methanol to porphyra-334 were used to assess the quantum yield of the triplet production in aqueous solution, affording an upper limit of 3 % [31]. This result accounts for the low probability of triplets to generate reactive intermediates which might start further chemical reactions, in agreement with the lack of radical detection previously reported [36].

The triplet–triplet absorption spectrum of porphyra-334 was determined by sensitization with benzophenone and consisted of a broad band centered at around 420 nm. Similar results were obtained for shinorine and palythine, both sensitized by acetone [31, 35].

The energy of the triplet state was estimated from the evaluation of the rate constants for the energy transfer processes with different donors with variable triplet energies. Thus, triplet energy for porphyra-334 in water solution is delimited to be <250 kJ mol^{-1} whereas the triplet energy for palythine is approximately 330 kJ mol^{-1} [28, 35]. In the cases of shinorine and palythine, small quantum yields for triplet formation were also obtained ($\Phi_T < 5 \times 10^{-2}$) by using acetone as sensitizer. The triplet life times were determined under the same conditions. Thus, for porphyra-334 a value of 14 μs was obtained, while shinorine and palythine yielded 11 μs and 9 μs, respectively.

Non radiative deactivation

Photoacoustic calorimetry studies allowed the direct quantification of non-radiative deactivation pathways of the excited species [31]. Laser induced experiments at two different temperatures on porphyra-334 and shinorine aqueous solutions led to conclude that around 98 % of the absorbed energy was promptly dissipated as heat to the environment. For palythine, analogous determinations showed that *ca*. 90 % of the light energy is transferred to the medium as heat [35]. Thus, these compounds proved to have all the features that should be desirable for an ideal sunscreen from the photophysical point of view.

Photochemical properties

Photostability

As previously stated, MAAs have been suggested to play a number of different roles. While some of them are probably speculative, the photoprotective capabilities of these species have been analyzed in detail. The role in UV-protoprotection is supported by several characteristics that turn MAAs into compounds capable of dealing very efficiently with the potentially damaging effects of radiation. First, MAAs evidence a strong UV absorption in the UVA-UVB region of the spectrum as described in the previous section. Second, these compounds also show a very low fluorescence emission yield. Nevertheless, a number of natural compounds can also share these two properties. In the case of MAAs, these features are also accompanied by a high photostability that greatly increases their relevance.

Preliminary results on the photostability of MAAs were obtained through UV irradiation of eggs of the green sea urchin [32]. The concentration of shinorine (the predominant MAA in the samples) remained unaltered for short-term UV irradiation in vivo and long-term exposure in vitro as determined by HPLC. Also, extracts from the red alga *Gracilaria cornea* (mainly containing porphyra-334 and shinorine) showed no change in the in vitro absorption properties when exposed to UVB as demonstrated by UV absorption spectroscopy [37]. More recently, a number of reports by Rastogi and Incharoensakdi have addressed the stability of MAAs occurring in different cyanobacteria species with the purpose of evaluating the photoprotective ability of these ancient organisms against damaging effects of UV radiation. They showed that palythine, asterina and a compound designated as M-312 which could not be identified, all present in a partially purified aqueous extract from *Lyngbya* sp., were highly resistant to UVB [38]. Similarly, the absorbance of mycosporine-glycine obtained from the cyanobacterium *Arthrospira* (*Spirulina*) was found to slightly decrease upon exposure to different regions of UV radiation [39]. Shinorine and a non identified compound with maximal absorbance at 307 nm were detected in *Gloeocapsa* sp. isolated from the autotrophic biofilm covering stone monuments. The extent of degradation of the compounds in a partially purified extract under spectrally differentiated UV sources was also qualitatively assessed by HPLC analysis [40].

Further detailed studies on diverse MAAs provided quantitative evidences on the high degree of photostability of these compounds in vitro. The photodegradation of aqueous solutions of porphyra-334 was explored by following the spectral changes as a function of time when irradiating with a medium-pressure Hg lamp [28]. The photodecomposition quantum yield was determined to be $\Phi_R = 1.9 \times 10^{-4}$ under N_2 atmosphere and $\Phi_R = 3.4 \times 10^{-4}$ in 1 atm O_2-equilibrated aqueous solutions, by using valerophenone as actinometer. On

one hand, this MAA was found also to be very photostable. On the other hand, the small effect of oxygen in the photodecomposition quantum yield seems to suggest a scarce contribution of the triplet state in the photochemistry of these compounds. In agreement with the results from photoacoustic calorimetry described above, shinorine and porphyra-334 dissipate most of the absorbed energy as heat into the environment consistently with the very low photodecomposition quantum yield [28, 31]. Palythine was also studied in order to confirm its photostability [35]. Continuous irradiation at 320 nm (absorption maximum) of aqueous solutions showed no significant changes in the pH nor the absorbance. The photodecomposition quantum yield for this MAA was found to be $\Phi_R = 1.2 \times 10^{-5}$.

These results suggest that the photostability of MAAs is related to their core structure and the variability of substituents among different MAAs only have a minor effect on the photochemical properties. Interestingly, the photostability of these compounds is also maintained when incorporated in more complex structures. This is illustrated by mycosporine-glutaminolglucoside (Fig. 3) [41], a mycosporine metabolite present in several yeast species, which was also found to be very photostable ($\Phi_R = 1.2 \times 10^{-5}$) most probably due to the mycosporine moiety [42].

Photoisomerization

The high photostability of MAAs seems to be caused by the general structure of aminocyclohexenimine or aminocyclohexenone. Beyond this common moiety, the different substituents in the basic core of MAAs appear to be related with the metabolic routes but most of them have a minor effect in the photophysical and photochemical properties of these compounds. The amino and alcohol groups directly bonded to the chromophore only affect the wavelength of absorption while keeping the photostability almost unchanged. The rest of substituents do not have any relevant influence in the chromophore. Acid, amino, and alcohol groups present in the lateral chains have probably their origin in the biosynthetic routes and seem to have minor effects on the solubility. However, some differences may arise when the substituents directly affect the chromophore. Among the different isolated MAAs, this may happen in the pair palythene–usujirene (Fig. 1) [33]. In these two compounds, an additional double C=C bond is conjugated with the common chromophore. Thus, the absorption occurs at higher wavelengths: 360 nm for palythene and 357 nm for usujirene, in contrast with the absorption at 320 nm for palythine, the equivalent MAA without the C=C bond. Besides this evident consequence of the extra double bond, a higher photoreactivity was also expected.

In a careful study of the reactivity of this couple of compounds, continuous irradiation of usujirene at 366 nm and HPLC quantitative analysis allowed for the evaluation of its photodecomposition quantum yield, amounting $\Phi_R = 2.9 \times 10^{-5}$ [43]. However, most of the disappearance of usujirene was due to the *cis-trans* isomerization of the exocyclic C=C double bond to yield palythene with an only slightly lower quantum yield ($\Phi_{iso} = 1.7 \times 10^{-5}$). Thus, most of the reacting usujirene leads to the formation of palythene, its photostable isomer. Under these conditions, a photostationary state composed by palythene and usujirene (11:1) was

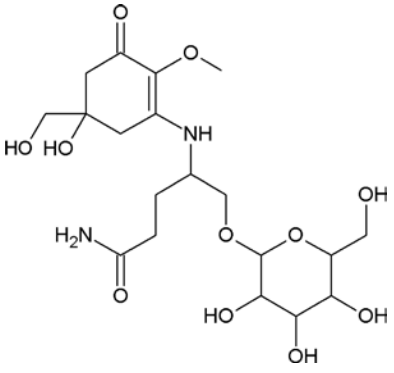

Fig. 3: Molecular structure of mycosporine-glutaminolglucoside.

found, probably explained by the intrinsic higher stability of the *trans* C=C double bond in palythene. Thus, usujirene and palythene undergo photoisomerization as an additional reactivity in the excited state. This reactive pathway converts one isomer into the other affecting the mixture composition while keeping the global photoprotective capacities.

Photosensitized processes

As described in the previous sections, the high photostability of MAAs is a key aspect for their photoprotective capability together with the strong absorption in the relevant UV regions. From a purely photochemical point of view this implies that direct absorption of a photon populates excited electronic states of singlet multiplicity that eventually decay to the ground state mainly through non-reactive and non-radiative pathways. However, it should be noted that other reactive possibilities may also influence the protection achieved in vivo. Among them, the photosensitized processes are viable photodegradation routes provided that different sensitizers may be available in biological media. For instance, flavin-mediated photodegradation of mycosporine glutamine leads to the formation of an aminocyclohexenone and 2-hydroxyglutaric acid [44]. This reactivity is independent of the pH but temperature and light wavelength have a clear effect. Thus, a mixture of photochemical and thermal degradation paths seems to be operating at the same time. Different sensitizers such as erythrosine, methylene blue or Rose Bengal (RB) are also effective.

Further comparative studies with up to seven different MAAs evidenced photosensitized decomposition in the presence of riboflavin, RB or simply natural seawater [45]. However very different decomposition rates were observed when RB (an efficient singlet oxygen source) and riboflavin (a photosensitizer) were used. A higher rate of photodecomposition was observed when riboflavin was present, this indicating that a type I photooxidation mechanism may be responsible for the degradation. Also, the requirement of a strong photosensitizer such as riboflavin and the low decomposition rates when other sensitizers are present further confirms the high photostability of MAAs even under indirect irradiation.

It was already mentioned that several MAAs have been the subject of detailed analysis in photosensitization experiments that enabled the characterization of their triplet states. In fact, neither porphyra-334 nor shinorine showed any transient absorption in laser flash photolysis measurements within the microsecond time range. In contrast, the triplet states were detected upon sensitization with benzophenone or 1-naphtalene-methanol for porphyra-334 and with acetone for shinorine [28, 31]. Palythine also forms triplets under sensitization with acetone [35].

The energy of these triplets states were respectively estimated by considering the efficiency of the energy transfer in relation with the triplet energy of the donor. These triplet energy values are relevant for the discussion of the complementary role of MAAs that consists of avoiding the formation of pyrimidine dimmers [46]. These species are associated with molecular damages caused in DNA through photochemical reactions. When thymine or cytosine bases absorb UV light, the formation of covalent linkages between two of these moieties by reactions localized on the C=C double bonds may take place [47]. Thus, MAAs were proposed not only to protect against the UV damage by direct absorption and filtering of the light, but also through quenching the excited state of thymine thus avoiding the formation of the dimers. However, as the value for the triplet energy of thymine in DNA was estimated to be 270 kJ mol^{-1} [48], it seems that this possibility could be ruled out in the case of palythine (triplet energy *ca*. 330 kJ mol^{-1}) as no energy transfer seems possible from the thymine excited state. In contrast, porphyra-334, with triplet energy of 250 kJ mol^{-1}, could quench the excited thymine and contribute to the photoprotection through this additional mechanism.

Gadusols

As already mentioned, gadusols are structurally and biosynthetically related to MAAs. Two metabolites are referred under this name: 3, 5, 6-trihydroxy-5-hydroxymethyl-2-methoxycyclohex-2-en-1-one (known as

gadusol) and 3,5-dihydroxy-5-hydroxymethyl-2-methoxycyclohex-2-en-1-one (usually called 6-deoxygadusol, 4-deoxygadusol or simply deoxygadusol, Fig. 1).

Gadusol has been found in fish ovaries and eye lenses, and together with deoxygadusol in eggs and larvae of various aquatic invertebrates [11, 49–52]. The antioxidant properties of the compounds are comparable to those of ascorbic acid and this issue seems to have attracted most interest some years ago [4, 11, 14, 53, 54]. However, the UV-screening properties of gadusol have recently received particular attention in reference to potential roles in marine organisms [55, 56]. In vitro studies about photoinduced processes of these molecules in solution are limited to a few publications [54, 57, 58]. The main findings of this research will be reviewed in the following sections.

Photophysical properties

UV-Vis absorption

The electronic absorption characteristics of gadusol extracted from marine fish roes were examined in different solvents. In water solution, the maximum shifts reversibly from 268 nm to 296 nm and the intensity increases on going from acidic to neutral pH [57]. Previous publications by Grant et al. [50] and by Bandaranayake et al. [51] report respectively the values 269 (12 400 M^{-1} cm^{-1}) and 264 nm (12 900 M^{-1} cm^{-1}) for the peak wavelength and maximal molar absorption coefficient, ε_{max}, of the band in the acidic medium. For the absorption band at higher pH the informed values for ε_{max} range from 21 800 to 22 750 M^{-1} cm^{-1} [11, 50, 51].

The effect of the pH on the absorption spectrum of the metabolite has been ascribed to the deprotonation of the enol form of the molecule (gadusol) to give the resonance-stabilized enolate (gadusolate) as depicted in Fig. 4 [11, 50, 57].

The solvent effect was evaluated for the enolic species in acetonitrile–water mixtures, various alcohols, 1,4-dioxane, and organic acids. A tendency to bathochromic shifts was observed for the absorption maxima with increasing polarity of the solvent, pointing to a relative stabilization of the excited state which suggests its π–π^* nature. The results are consistent with specific interactions involving hydrogen bonds between gadusol and the solvent molecules. Correlation of the data according to the Kamlet–Taft empirical approach indicates comparable contributions of the hydrogen donor and acceptor characters of such interactions, probably implying the hydroxylic and ketone groups of gadusol [57].

Radiative and non-radiative deactivations

Steady state fluorescence measurements evidenced no net emission from gadusol in acid water by excitation at 268 nm or from gadusolate under neutral pH by excitation at 296 nm [57].

Non-radiative relaxation pathways were quantified for gadusolate, the physiologically relevant species, in aqueous phosphate solution by photoacoustic calorimetry. The photoacoustic signals for gadusolate with laser excitation at 266 nm matched exactly those from the calorimetric reference; potassium dichromate dissolved in the same medium, no matter the temperature of the experiment (298 K or 283 K). This indicated that excited gadusolate promptly releases the complete amount of absorbed UV energy as heat to the surroundings.

No transient absorption was detected by direct laser flash photolysis of gadusolate at 266 nm that could be attributed to T–T transitions [57]. The result contrasts the production of stabilized triplets reported for

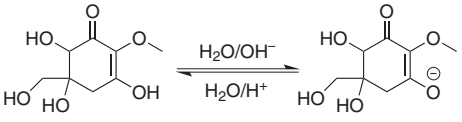

Fig. 4: Gadusol–gadusolate equilibrium.

β-carbon substituted α,β-unsaturated ketones [59]. However, in the case of gadusolate, the formation of long lived triplets is probably avoided under the competition with the extremely rapid internal conversion involving allowed $\pi \rightarrow \pi^*$ transitions.

Photochemical properties

Photostability

The photostability of both forms of gadusol in aqueous solution was assessed by monochromatic steady irradiation and chemical actinometry with phenylglyoxylic acid. The photodecomposition quantum yields amounted $\Phi_R = 3.6 \times 10^{-2}$ for gadusol at 254 nm and $\Phi_R = 1.4 \times 10^{-4}$ for gadusolate at 303 nm. No significant effect was found for the presence of oxygen on these yields [57]. Both values denote a high photostability, although the photodecomposition yield for the neutral form of gadusol is two orders of magnitude larger. Thus, the most photostable species from both is the anionic form, gadusolate, which dominates the acid base equilibrium under physiological pH. Moreover, gadusolate photodecomposition quantum yield compares better than gadusol's with the values for MAAs in solution [28, 31, 35]. This result accounts for the favorable conditions supporting a UV-screening role of the metabolite, particularly relevant in prebiotic environments.

Photosensitized processes

A series of laser flash photolysis studies on gadusolate in the presence of efficient triplet sensitizers were carried out in polar media and anoxic conditions by Arbeloa et al. [57]. The studies confirmed the ability of the natural molecule to react as a reductive quencher. The transient spectra obtained for experiments in methanol with excitation at 355 nm and benzophenone or acridine as sensitizers are consistent with the occurrence of electron transfer processes. In fact, the spectral features of benzophenone ion radical, and a neutral "C" radical from acridine were respectively evidenced in these studies.

On the other hand, RB was used as triplet donor in water solution with laser excitation at 532 nm. The kinetic analysis of the transient bands clearly showed the decrease of the absorbance of RB triplet state at 590 nm and the concomitant enhancement of the signal at 410 nm due to the semireduced form of the sensitizer. The time constant of the decay of triplet RB as a function of gadusolate concentration followed the Stern-Volmer dependence with a quenching rate constant $k_q = 2 \times 10^8\ M^{-1}\ s^{-1}$, thus below the diffusion limit in water. However, the presence of gadusolate at concentrations as large as 2.3×10^{-3} M did not affect the transient absorption spectrum of anthracene in methanol obtained by excitation at 355 nm. These findings were rationalized in terms of the following one electron transfer from gadusolate (Gad^-) to the triplet state sensitizer (^3Sens) yielding the sensitizer radical anion ($Sens^{\bullet -}$), and the neutral gadusol radical ($Gad^\bullet$):

$$Gad^- + {}^3Sens \rightarrow Sens^{\bullet -} + Gad^\bullet \quad (1)$$

An energetic analysis of reaction (1) requires taking into account the reduction potentials of the sensitizer and of gadusol, and the triplet energy of the sensitizer. On this basis, a less favourable thermodynamic balance explains the lack of reaction with anthracene triplets and predicts the feasibility of gadusol to quench natural sensitizers such as riboflavin. Thus, the reductive quenching reactivity of gadusol may be considered as one of the potential contributions to the antioxidant mechanisms involving the metabolite in biological environments.

Theoretical calculations

In spite of the enormous work accumulated about the location, biosynthesis and biological role of MAAs and related compounds as gadusol, very few reports on the chemical properties of these species obtained

by theoretical calculations have appeared. In fact, most of them are related with the determination of the chemical structures as a complement to the experimental techniques. For instance, the stereochemistry of porphyra-334 was explored by NMR using both experiments and theoretical calculations under the framework of the density functional theory (DFT) using the functional B3LYP and the standard 6-31G(d) basis set [26]. As the right stereochemical assignment could not be achieved by attending exclusively at the experimental data, theoretical NMR signals for up to nine different tentative structures for porphyra-334 were computed. A good agreement between the experimental and computational NMR data was found.

The structures of palythine, palythinol and asterine were also studied by high-resolution accurate-mass sequential mass spectrometry and theoretical calculations [60]. A similar level of theory was used (B3LYP functional together with the 6-31G + (d,p) basis set). All the calculations were performed in the gas phase. This may not be representative of the real structures in water solution, although this situation is closer to the experimental conditions used for the mass spectrometry. The combined experimental and computational study allowed for the explanation of the fragmentation pattern found for the different MAAs together with the proposal of molecular fragments previously unassigned. However, the information relative to the protonation sites available in the molecules should be taken with extreme caution as the real situation in water may be completely different. In a subsequent study, shinorine and porphyra-334 were analyzed following a similar methodology in negative ion mode [61].

The photochemistry of palythine [62] has been also subject of detailed theoretical calculations using the high-level CASPT2//CASSCF strategy [63] with an active space of 10 electrons in 7 orbitals, 6-31G* as the basis set and using the polarizable continuum medium (PCM) in order to include the solvent effects. First, the exact structure of the MAA in aqueous solution was explored. In physiological conditions both the neutral and protonated forms may be present (Fig. 5).

The computed UV spectra for both compounds show that the protonated form must be the major species in neutral aqueous solutions. Further exploration of the minimum energy paths (MEPs) describing the relaxation from the Franck–Condon region to the ground state recovery for both species proved the ultrafast deactivation of the excited state. Upon light absorption to S_2 in the neutral form or S_1 in the protonated palythine, easy and fast (barrierless) relaxation in the excited states potential energy surfaces allows for the recovery of the starting material. Thus, the light energy absorbed by the molecule is very efficiently dissipated as heat into the environment. This was the first direct proof of the effective photoprotective capabilities of MAAs (Fig. 6).

Also relevant for the photoprotective capabilities of MAAs in general and specifically for palythine is the fate of the molecule upon ground state recovery. Beyond the strong absorption in the relevant regions of the UV spectrum, the photostability is a key feature of an ideal photoprotective compound. This property has been invoked repeatedly for MAAs as continuous irradiation of these compounds usually does not imply a significant degree of decomposition (see above). The photostability of palythine was also explored using the same methodology. The computational data allowed for an explanation of this issue. Upon light absorption and relaxation in the excited state potential energy surface, a region is reached in which the energies of at least two potential energy surfaces are similar. This is known as conical intersection (CI) point and it is topologically defined as the geometry in which two potential energy surfaces have the same energy. From the CI point, population of the state of lowest energy is allowed and very fast. Thus, the ground state recovery takes place at CI points in which the excited state and the ground state have the same energy. The photoproduct

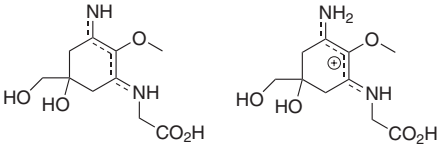

Fig. 5: Molecular structures for neutral (left) and protonated (right) palythine.

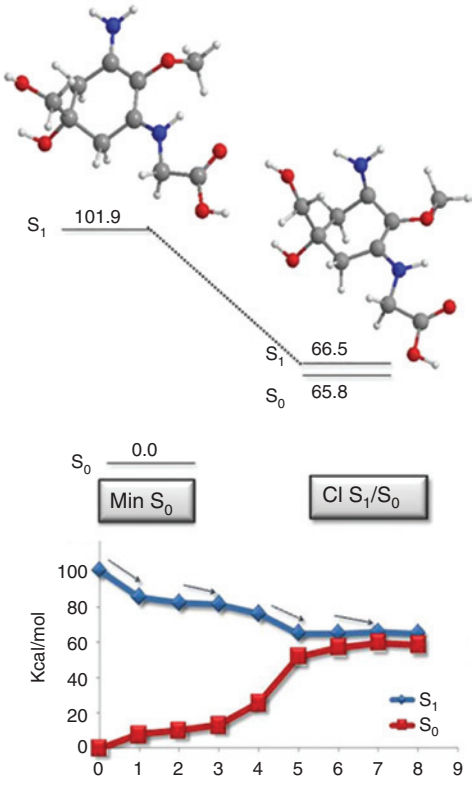

Fig. 6: Critical points along the potential energy surface and MEP for the palythine protonated form. Energies in kcal mol^{-1} relative to ground state minimum. Sampedro, D. *Phys. Chem. Chem. Phys*. **2011**, *13*, 5584. Reproduced by permission of the PCCP Owner Societies.

formation depends, among other factors, on the geometry of these CI points. For palythine, it was found that after the CI point is reached, two different possibilities arise (Fig. 7). On one hand, the starting material can be recovered unchanged. On the other hand, a conformer only slightly (+1.5 kcal mol^{-1}) more unstable is formed. This conformer will produce the more stable isomer once the equilibration in the ground state takes place. Thus, in both cases, the final photoproduct formation implies the recovery of the starting material in agreement with the experimentally determined photostability. These results, beyond the mechanistic explanation of the experimental observations, allow for the generalization of the relevant features required to generate an effective photoprotector.

A similar study has been recently published on the photochemistry of gadusol [58]. The CASPT2//CASSCF methodology with an active space of 16 electron in 12 orbitals allowed for the detailed theoretical analysis of the photochemistry of this molecule. In this work, PCM was used to model the solvent and the influence of the basis set was checked with the 6-31G* and ANO-L-VDZ basis sets. The experimental photophysical features

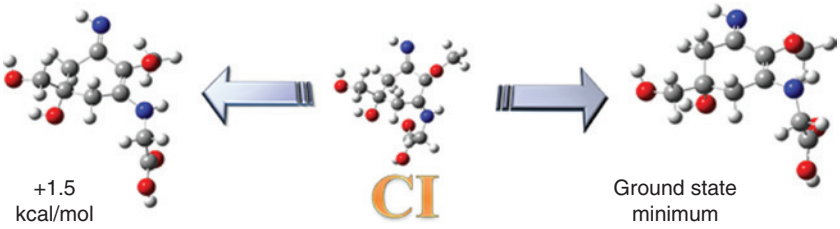

Fig. 7: S_1/S_0 conical intersection geometry and conformers obtained after ground state relaxation for the palythine neutral form. Sampedro, D. *Phys. Chem. Chem. Phys*. **2011**, *13*, 5584. Reproduced by permission of the PCCP Owner Societies.

found for gadusol in different solvents and pH values could be computationally explained. Thus, the bathochromic shift was observed as the polarity of the solvent increases and the major species in solution was determined as function of the pH: gadusol in acidic solution and gadusolate in neutral solutions. Also, different deprotonation sites were considered (Fig. 8).

The theoretical results show that both gadusolate and gadusol rapidly deactivate and dissipate light energy as heat very efficiently. This effect is especially relevant for gadusolate as it features a stronger absorption band. In addition, no intermediates were found along the different computed reaction paths. This is in agreement with the lack of fluorescence experimentally found. As it happens with palythine, the starting material is mainly recovered after irradiation, according to the low decomposition quantum yields observed. In turn, this implies that these molecules present a very high photostability.

The geometries of the CI points of palythine and gadusol show some similar features in agreement with the comparable role that these compounds play in different organisms (Fig. 9).

In the case of palythine (Fig. 9, left), the S_1/S_0 CI features a main deformation corresponding with an out-of-plane movement of the imine moiety. At the same time, the adjacent carbon atoms approach to each other and the alkene moiety remains almost planar. Subsequent relaxation on the ground space following the directions of the vectors of the branching space recovers the starting material.

For gadusol (Fig. 9, right), the main molecular distortions are also the breakage of the π system and the out-of-plane movement of the oxygen atoms in the carbonyl and alcohol groups of the chromophore. Then, deactivation in the ground state recovers also the initial structure.

Thus, high-level theoretical calculations show that the photoprotective mechanisms found for gadusol and MAAs are very similar. This is an indirect proof of the working hypothesis that suggests the relationship between gadusol and MAAs in terms of metabolic routes. Even more, these two types of compounds have been proposed to be different steps in the evolution of natural photoprotective compounds [8].

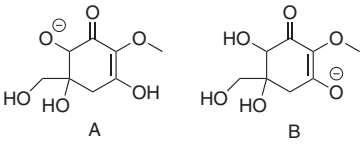

Fig. 8: Computed anionic species for gadusol.

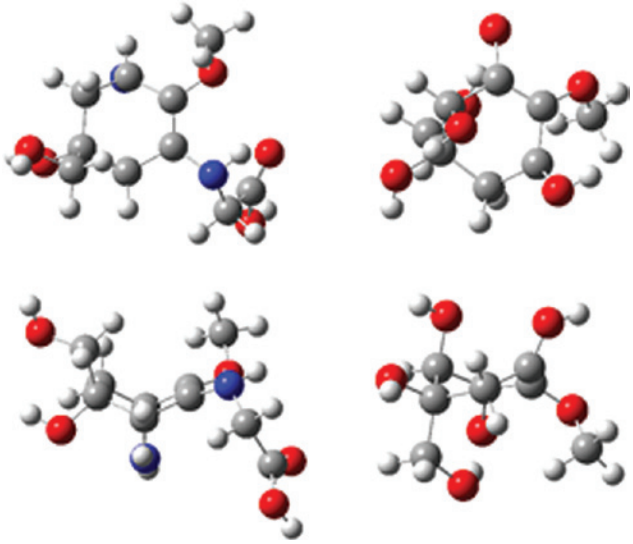

Fig. 9: Computed conical intersection points for palythine (left) and gadusol (right).

Design of new sunscreens

As shown in the previous sections, MAAs meet most of the required characteristics for an ideal sunscreen. However, all the described studies on these compounds were carried out on samples extracted from natural sources. While significant amounts of MAAs occur in various types of organisms, these natural sources present many disadvantages that restrain their practical applications. For instance, MAAs are relatively unstable once they have been extracted from the organism and, more importantly, only very small quantities can be obtained from natural sources. The instability is due to a dehydration process which involves the hydrolysis of the amine in C-3 and the elimination of hydroxyl group in C-5 position [33, 64]. These reactions destroy the chromophore and prevent any further use of the resulting products as photoprotectors.

To try to solve these drawbacks, several synthetic efforts have been done to obtain MAAs through a synthetic pathway. Unfortunately, many of them did not lead to any favorable results.

Only two examples of a total synthesis for MAAs have appeared in the literature [65, 66]. In both, the synthesis of MAAs was carried out by using quinic acid as the starting material. The synthetic pathway is quite similar in both cases, involving a common part with minor modifications in the route. A schematic pathway for mycosporine-glycine is shown in Fig. 10.

As seen, this synthetic route involves about 15 steps with a very small total yield, about 1 % with respect to the initial quinic acid. These two factors make this pathway unpractical to obtain large amounts of MAA and inhibit any attempt to use those compounds in commercial applications.

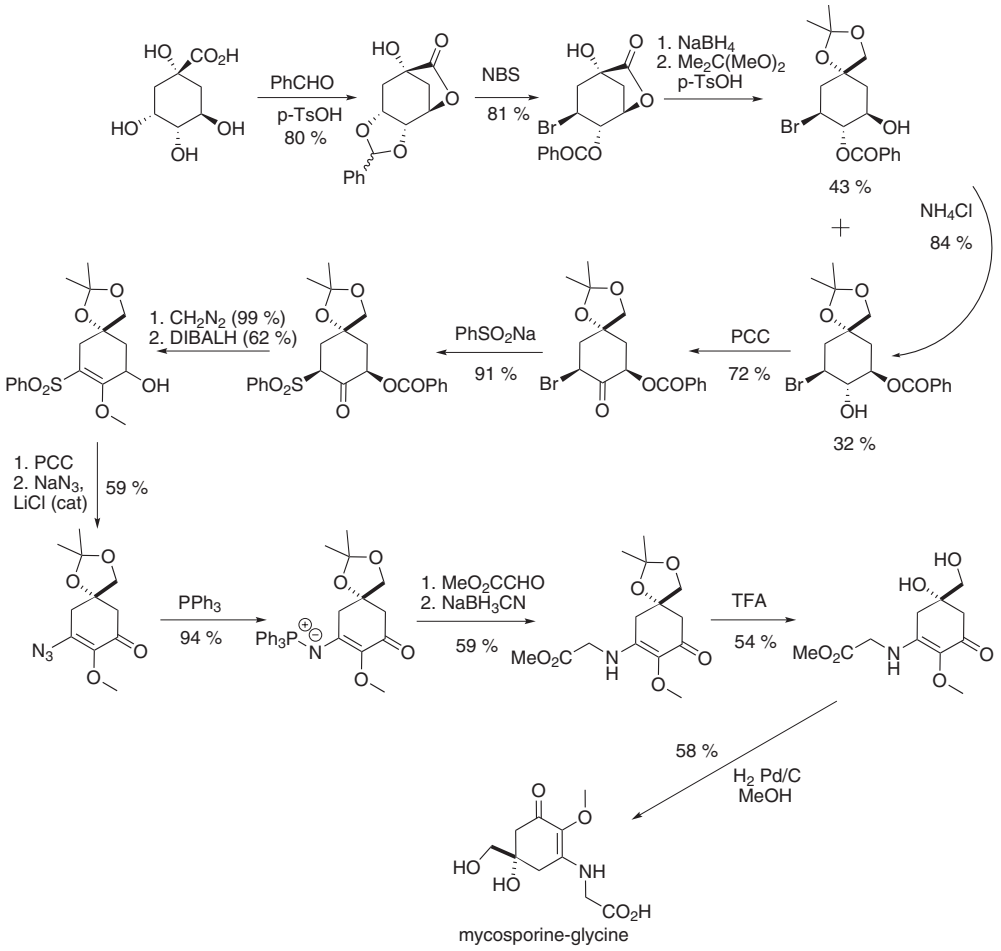

Fig. 10: Scheme of direct synthetic pathway described in 1995 [66].

On the other hand, the relevant photochemical properties of MAAs seem to be restricted to a very specific central core. Thus, a structural simplification while keeping the important features may be reasonable. In this sense, some attempts in the field of aminocyclohexenone-MAAs have been reported. One of these simplifications is shown in Fig. 11.

The first attempt described to prepare a synthetic simplified MAA was reported by Dunlap et al. in [67]. They proposed the structural simplification shown in Fig. 11 and studied the effect of different substituents in some positions. This was carried out in three consecutive generations of compounds in which different structural modifications were included.

For the first generation, a new synthetic method was proposed. It was based in the high-pressure hydrogenation of pyrogallol over a Raney nickel catalyst to give dihydro-pyrogallol [68], which is then converted to 3-hydroxy-2-methoxycyclohex-2-enone [69]. The treatment with primary amines yields by condensation 3-alkylamino-2-methoxycyclohexen-2-enones with good yields. The synthetic route shown in Fig. 12 affords for the preparation of compounds structurally similar to mycosporine-glycine. Also this pathway is reported in a previous Dunlap patent [70] which includes the synthesis of five-member ring analogues.

The study of the light absorption properties reveals that these derivatives have UV absorption maximums in the range of 309–312 nm for monosubstituted amines and 318–322 nm in the case of secondary amines. However, these disubstituted aminoderivatives are not useful in practical applications due to their high instability, as they are prone to hydrolysis and oxidative decomposition [71].

The influence of the C-2 substituent in the electronic behavior of the chromophore was also subject to exploration (Fig. 13). Removal of the 2-methoxy group gave enaminoketones with absorbance maximum at shorter wavelengths, in the range of 290–296 nm. In the case of alkyl C-2 substitution a small red shift of *ca*. 5 nm can

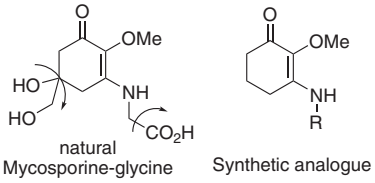

Fig. 11: Strategy for the design of simplified structures.

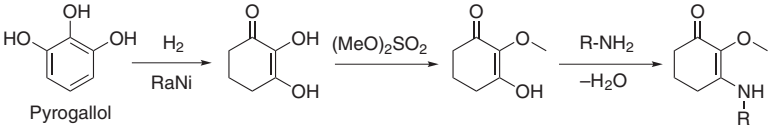

Fig. 12: Schematic synthesis from pyrogallol.

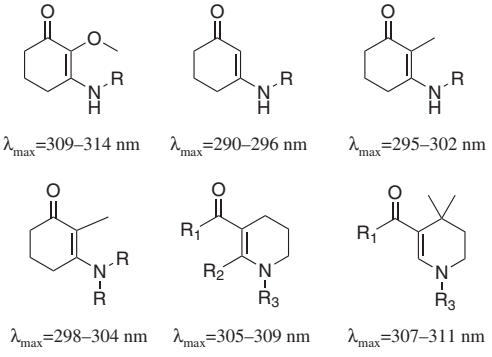

Fig. 13: Substituent effect in second and third generation of MAA analogues.

be achieved. Condensation products of 2-methyl analogues with secondary amines yielded absorption at longer wavelengths (298–304 nm). These structural modifications are under patent protection [72, 73].

The third generation of MAA analogues reported by Dunlap implied the modification of the six membered ring (Fig. 13). This modification prevents the hydrolytic cleavage of the enaminone, but in contrast the oxidative decomposition of the tetrahydropyridine ring can be relevant. This oxidation may be related with radical processes at the α-carbons and can be further limited by removal of the alkyl substituents at the 2-position in the tetrahydropyridine ring. Thus, the presence of *gem*-dimethyl groups is needed. These methyl groups block the radical processes responsible of the oxidation and restrict the rotation of the alkanoyl group, which in turn induces a bathochromic shift. The steric hindrance and subsequent structure rigidity increases delocalization of the chromophore and extends the absorption band to 307–311 nm. This third generation of compounds is also protected under patent [73].

Other different synthetic strategies and compounds are also under patent protection. In one of them, different aminocyclohexenones are proposed as drugs against oxidative stress [74].

In a recent and very relevant patent [75], the use of natural MAAs in cosmetical preparations is claimed. This implies the incorporation of natural MAAs in commercial applications. Although a synthetic methodology is suggested, only the retrosynthesis is provided, with no specific details of the preparation. The retrosynthesis consists of seven or eight steps with only indicative reaction conditions (Fig. 14).

The first retrosynthetic step may be carried out by dihydroxylation of the previous compound **2** with OsO_4 or sodium hypochlorite followed by hydrolysis. **2** may be done by treatment with a primary amine of compounds **3** or **4**. **4** is an intermediate that may be obtained by reaction of **3** with a chlorinating agent like Vilsmeier's reagent. Compound **3** could be achieved by condensation of **5** with a primary amine. **5** may be prepared by methylation of **6**, which may be obtained by reaction of **7** with an aqueous solution of cupric chloride. Finally, compound **7** may be done by sequentially silylation, Birch reduction and protodesilylation reactions from **8**.

However, no examples of total synthesis of imino-mycosporines have been reported yet. To date, only the synthesis of aminocyclohexenones has been described and no examples of aminocyclohexenimines substituted in C-2 with any group different than hydrogen have appeared. This fact was already noted by Nguyen et al. in [21].

In contrast, some examples of aminocyclohexenimines non-substituted in C-2 can be found in the literature. Vinamidinium salts can be prepared by treatment of 1,3-cyclohexanedione with two equivalents of an aromatic amine in the presence of *p*-toluensulfonic acid [76]. Also, aminocyclohexenones can be treated by an alkylating agent to yield 3-alkoxy-2-cyclohexen-1-ylidene salts which subsequently reacts with amines to give the vinamidinium salts (Fig. 15) [77].

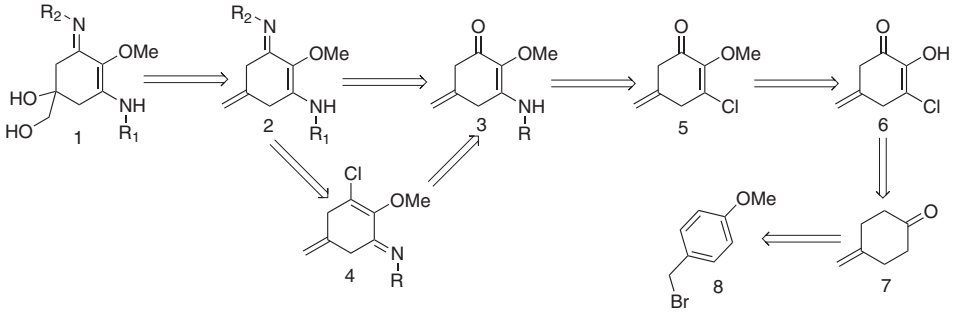

Fig. 14: Retrosynthesis proposed in the WO0239974A1 patent.

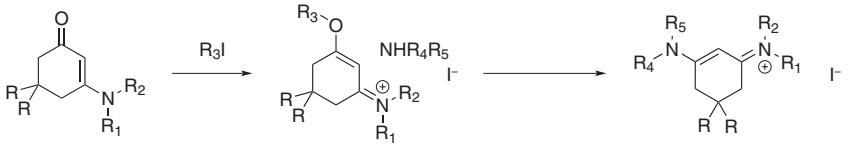

Fig. 15: Synthesis of rigid core vinamidinium salts.

These compounds are proposed to be photostable due to the similarity between iminoderivatives and MAAs but no detailed information was reported.

Conclusions

The location, synthesis and potential roles of MAAs and related compounds in biological systems have been intensively researched since their discovery. However, some key features of these species are still on debate. For instance, various evolutionary aspects linking MAAs and gadusols or the biosynthesis of these compounds in different organisms are not yet completely understood. Nonetheless, much effort remains to be done to unveil the chemistry of these metabolites. Both as antioxidants and photoprotective species, MAAs and gadusols have shown an impressive potential in living organisms. A detailed investigation of the chemical aspects at the molecular level behind these features could provide not only much insight into the biological relevance of these compounds, but it also could be useful for the development of new compounds with improved performance. The exceptional properties of MAAs as sunscreens in living organisms could be translated to a new generation of commercial applications for human health care. The protection against the damaging effects of solar UV light is becoming more and more important as the figures for solar exposure skin cancers are steadily increasing. However, before this could be achieved, much work must be carried out in many different areas. A careful screening of relevant living organisms will lead most probably to the discovery of new examples of MAAs and gadusols, and even other types of related metabolites. The photochemical and photophysical studies of these compounds should be generalized in order to obtain a deeper insight into the general mechanism of photoprotection. Finally, the efficient, versatile and easy synthesis of MAAs analogues will facilitate the use of some of these compounds in commercial applications.

Acknowledgments: M.S.C. thanks the financial support from CONICET (PIP-0211) and UNMDP (15-E611). R. L. and D. S. thank the Spanish MICINN (CTQ 2014-59650-P).

References

[1] R. P. Sinha, S. P. Singh, D.-P. Häder. *J. Photochem. Photobiol. B*. **89**, 29 (2007).
[2] E. P. Balskus, C. T. Walsh. *Science* **329**, 1653 (2010).
[3] A. Oren, N. Gunde-Cimerman. *FEMS Microbiol. Lett.* **269**, 1 (2007).
[4] J. M. Shick, W. C. Dunlap. *Ann. Rev. Phys.* **64**, 223 (2002).
[5] N. Korbee, P. Huovinen, F. L. Figueroa, J. Aguilera, U. Karsten. *Mar. Biol.* **146**, 645 (2005).
[6] C. E. Kicklighter, M. Kamio, L. Nguyen, M. W. Germann, C. D. Derby. *Proc. Nat. Ac. Sci.* **108**, 11494 (2011).
[7] W. M. Bandaranayake. *Nat. Prod. Rep.* **15**, 159 (1998).
[8] Q. Gao, F. Garcia-Pichel. *Nat. Rev. Micro.* **9**, 791 (2011).
[9] J. I. Carreto, M. O. Carignan. *Mar. Drugs.* **9**, 387 (2011).
[10] E. M. Arbeloa, M. J. Uez, S. G. Bertolotti, M. S. Churio. *Food Chem.* **119**, 586 (2010).
[11] P. A. Plack, N. W. Fraser, P. T. Grant, C. Middleton, A. I. Mitchell, R. H. Thomson. *Biochem. J.* **199**, 741 (1981).
[12] A. Starcevic, W. C. Dunlap, J. Cullum, J. M. Shick, D. Hranueli, P. F. Long. *PLoS ONE.* **5**, e13975 (2010).
[13] F. Garcia-Pichel. *Orig. Life Evol. Biosph.* **28**, 321 (1998).
[14] W. C. Dunlap, J. M. Shick, Y. Yamamoto. in *Free Radicals in Chemistry, Biology and Medicine*, S. T. T. Yoshikawa, Y. Yamamoto, Y. Naito (Eds.), pp. 200–214, OICA International, London (2000).
[15] S. Khosravi, S. Khodabandeh, N. Agh, M. Bakhtiarian. *Photochem. Photobiol.* **89**, 400 (2013).
[16] R. P. Rastogi, A. Incharoensakdi. *Plant Physiol. Biochem.* **70**, 7 (2013).
[17] R. P. Rastogi, R. P. Sinha, S. H. Mohc, T. K. Lee, S. Kottuparambil, Y-J. Kim, J-S. Rhee, E-M. Choi, M. T. Brown, D-P. Häder, T. Han. *J. Photochem. Photobiol. B.* **141**, 154 (2014).
[18] R. M. Lucas, M. Norval, R. E. Neale, A. R. Young, F. R. de Gruijl, Y. Takizawa, J. C. van der Leun. *Photochem. Photobiol. Sci.* **14**, 53 (2015).
[19] K. Morabito, N. C. Shapley, K. G. Steeley, A. Tripathi. *Int. J. Cosmet. Sci.* **33**, 385 (2011).
[20] D. Schmid, C. Schürch, F. Zülli, H.-P. Nissen, H. Prieur. *SOFW-J.* **129**, 2 (2003).

[21] K. H. Nguyen, M. Chellet-Krugler, N. Gouault, S. Tomasi. *Nat. Prod. Rep.* **30**, 1490 (2013).
[22] R. Pallela, Y. Na-Young, S.-K. Kim. *Mar. Drugs.* **8,** 1189 (2010).
[23] T. Bjornland. *Monographs on oceanographic methodology.* 578 (1997).
[24] D. Uemura, C. Katayama, A. Wada, Y. Hirata. *Chem. Lett.* **9**, 755 (1980).
[25] Z. Zhang, Y. Tashiro, S. Matsukawa, H. Ogawa. *Fish. Sci.* **71**, 1382 (2005).
[26] M. Klisch, P. Richter, D.-P. Häder, W. Bauer. *Helv. Chim. Acta.* **90**, 488 (2007).
[27] H. A. Staab, T. Saupe. *Angew. Chem. Int. Ed. Engl.* **27**, 865 (1988).
[28] F. R. Conde, M. S. Churio, C. M. Previtali. *J. Photochem. Photobiol. B.* **56**, 139 (2000).
[29] A. H. Gröniger, D.-P. *Recent Res. Devel. Photochem. Photobiol.* **4**, 247 (2000).
[30] S. Takano, A. Nakanishi, D. Uemura, Y. Hirata. *Chem. Lett.* **8**, 419 (1979).
[31] F. R. Conde, M. S. Churio, C. M. Previtali. *Photochem. Photobiol. Sci.* **3**, 960 (2004).
[32] N. L. Adams, J. M. Shick. *Photochem. Photobiol.* **64**, 149 (1996).
[33] S. Takano, D. Uemura, Y. Hirata. *Tetrahedron Lett.* **26**, 2299 (1978).
[34] Y. Hirata, D. Uemura, K. Ueda, S. Takano. *Pure Appl. Chem.* **51**, 1875 (1979).
[35] F. R. Conde, M. S. Churio, C. M. Previtali. *Photochem. Photobiol. Sci.* **6**, 669 (2007).
[36] J. M. Shick, W. C. Dunlap, R. Buettner. in *Free Radicals in Chemistry, Biology and Medicine,* T. Yoshikawa, S. Toyokuni, Y. Yamamoto, Y. Naito, (Eds.), pp. 215–228, OICA International, London (2000).
[37] R. P. Sinha, M. Klisch, A. Gröniger, D.-P. Häder. *Environ. Exp. Bot.* **43**, 33 (2000).
[38] R. P. Rastogi, A. Incharoensakdi. *FEMS Microbiol. Ecol.* **87**, 244 (2014).
[39] R. P. Rastogi, A. Incharoensakdi. *Photochem. Photobiol. Sci.* **13**, 106 (2014).
[40] R. P. Rastogi, A. Incharoensakdi. *J. Photochem. Photobiol. B.* **130**, 287 (2014).
[41] R. Sommaruga, D. Libkind, M. van Broock, K. Whitehead. *Yeast.* **21**, 1077 (2004).
[42] M. Moliné, E. M. Arbeloa, M. R. Flores, D. Libkind, M. E. Farías, S. G. Bertolotti, M. S. Churio, M. R. Broock. *Rad. Res.* **175**, 44 (2011).
[43] F. R. Conde, M. O. Carignan, M. Sandra Churio, J. I. Carreto. *Photochem. Photobiol.* **77**, 146 (2003).
[44] J. Bernillon, M. L. Bouillant, J. L. Pittet, J. Favre-Bonvin, N. Arpin. *Phytochemistry.* **23**, 1083 (1984).
[45] K. Whitehead, J. I. Hedges. *J. Photochem. Photobiol. B.* **80**, 115 (2005).
[46] T. Misonou, J. Saitoh, S. Oshiba, Y. Tokitomo, M. Maegawa, Y. Inoue, H. Hori, T. Sakurai. *Mar. Biol.* **5**, 194 (2003).
[47] S. E. Whitmore, C. S. Potten, C. A. Chadwick, P. T. Strickland, W. L. Morison. *Photodermatol. Photoimmunol.Photomed.* **17**, 213 (2001).
[48] F. Bosca, V. Lhiaubet-Vallet, M. C. Cuquerella, J. V. Castell, M. A. Miranda. *J. Am. Chem. Soc.* **128**, 6318 (2006).
[49] F. Chioccara, A. Delia Gala, M. De Rosa, E. Novellino, G. Prota. *Bull. Soc. Chim. Bel.* **89**, 1101 (1980).
[50] P. T. Grant, P. A. Plack, R. H. Thomson. *Tetrahedron Lett.* **21**, 4043 (1980).
[51] W. M. Bandaranayake, D. J. Bourne, R. G. Sim. *Comp. Biochem. Physiol., Part B: Biochem. Mol. Biol.* **118**, 851 (1997).
[52] P. T. Grant, C. Middleton, P. A. Plack, R.H.Thompson. *Comp. Biochem. Physiol.* **80B**, 755 (1985).
[53] E. M. Arbeloa, M. O. Carignan, F. H. Acuña, M. S. Churio, J. I. Carreto. *Comp.Biochem. Physiol. B.* **156**, 216 (2010).
[54] E. M. Arbeloa, C. L. Ramírez, R. A. Procaccini, M. S. Churio. *Nat. Prod. Commun.* **7**, 1211 (2012).
[55] M. J. Bok, M.L. Porter, A. R. Place, T. W. Cronin. *Current Biology* **24**, 1636 (2014).
[56] J. Colléter, D. J. Penman, S. Lallement, C. Fauvel, T. Hanebrekke, R. D. Osvik, H. C. Eilertsen, H. D'Cotta, B. Chatain, S. Peruzzi. *PLoS ONE.* **9**, e109572 (2014).
[57] E. M. Arbeloa, S. G. Bertolotti, M. S. Churio. *Photochem. Photobiol. Sci.* **10,** 133 (2011).
[58] R. Losantos, M. S. Churio, D. Sampedro. *Chemistry Open* **4**, 155 (2015).
[59] D. I. Schuster, D. A. Dunn, G. E. Heibel, P. B. Brown, J. M. Rao, J. Woning, R. Bonneau. *J. Am. Chem. Soc.* **113**, 6245 (1991).
[60] K. H. M. Cardozo, R. Vessecchi, V. M. Carvalho, E. Pinto, P. J. Gates, P. Colepicolo, S. E. Galembeck, N. P. Lopes. *Int. J. Mass Spectrom.* **273**, 11 (2008).
[61] K. H. M. Cardozo, R. Vessecchi, S. E. Galembeck, T. Guaratini, P. J. Gates, E. Pinto, N. P. Lopes, P. Colepicolo. *J. Braz. Chem. Soc.* **20**, 1625 (2009).
[62] D. Sampedro, *Phys. Chem. Chem. Phys.* **13**, 5584 (2011).
[63] D. Sampedro. in *Photochemistry: UV/VIS Spectroscopy, Photochemical Reactions and Photosynthesis,* K. J. Maes, J. M. Willems (Eds.), Nova Science Publishers, New York (2011).
[64] I. Tsujino, K. Yabe, I. Sekikawa, N. Hamanaka. *Tetrahedron Lett.* **16**, 1401 (1978).
[65] J. D. White, J. H. Cammack, K. Sakuma. *J. Am. Chem. Soc.* **111**, 8970 (1989).
[66] J. D. White, J. H. Cammack, K. Sakuma, G. W. Rewcastle, R. K. Widener. *J. Org. Chem.* **60**, 3600 (1995).
[67] W. C. Dunlap, B. E. Chalker, W. M. Bandaranayake, J. J. W. Won. *Int. J. Cosmetic Sci.* **20**, 41 (1998).
[68] B. Pecherer, L. M. Jampolsky, H. M. Wuest. *J. Am. Chem. Soc.* **70**, 2587 (1948).
[69] W. Mayer, R. Bachman, F. Kraus. *Chem. Ber.* **88**, 316 (1955).
[70] W. C. Dunlap, B. E. Chalker, ES patent 8801184, Filed 9 October 1985, Issued 30 April 1986.
[71] K. Dixon, J. V. Greenhill. *J. Chem. Soc. Perkin II.* **2**, 164 (1974).
[72] G. Bird, N. Fitzmaurize, W. C. Dunlap, B. E. Chalker, W. M. Bandaranayake, International patent WO 88/02251, Filed 25 September 1986, Issued 7 April 1987.

[73] P. J. Chalmers, N. Fitzmaurice, D. J. Rigg, S. H. Thang, G. Bird, International patent WO 90/09995, Filed 23 February 1990, Issued 27 December 1991.
[74] E. Napolitano, S. Basagni, S. Trasciatti, European patent EP2371816A1, Filed 1 April 2010, Issued 5 October 2011.
[75] C. Llewellyn, E. Galley, International patent WO2002039974, Filed 16 November 2001, Issued 23 May 2002.
[76] J. M. Kim, J. E. Na, C. G. Lee, J. N. Kim. *Bull. Kor. Chem. Soc.* **25**, 163 (2004).
[77] D. L. Ostercamp, Y. Dinh, D. Graff, S. Wiles. *J. Org.Chem.* **68**, 3099 (2003).